Chemical Data Collections 28 (2020) 100456

Contents lists available at ScienceDirect

Chemical Data Collections

journal homepage: www.elsevier.com/locate/cdc

Synthesis and spectroscopic characterization of rhodanine azo dyes as selective chemosensors for detection of iron(III)

Dana Akram [a], Ismail A. Elhaty [b,*], Shaikha S. AlNeyadi [a,*]

[a] Department of Chemistry, College of Science, UAE University, P.O. Box 15551, Al-Ain, United Arab Emirates
[b] Department of Nutrition and Dietetics, School of Health Sciences, Istanbul Gelisim University, Istanbul, Turkey

ARTICLE INFO

Article history:
Received 13 May 2020
Revised 5 June 2020
Accepted 8 June 2020
Available online 12 June 2020

Keywords:
IR
NMR
Synthesis
Rhodanine
Fe^{3+} sensing
UV/vis spectrometry

ABSTRACT

As the presence of (Fe^{3+}) is strongly associated with many environmental and biomedical analysis, effective sensing methods are of great importance for monitoring Fe^{3+} levels in these systems. In this study, we synthesized a new rhodanine-based azo dye (**4d**) and compared it with compound (**4c**) which showed the best sensitivity and selectivity among our previously reported compounds. The interaction behaviors with Fe^{3+} ions using UV/vis, fluorescence, IR, and NMR spectrometric techniques were investigated. The spectroscopic characterization revealed that azo **4d** showed high affinity towards Fe^{3+} ions with association constant of 5.35×10^8 M^{-1}. Furthermore, it showed high sensitivity towards Fe^{3+} ions with detection limit of 7.05 µM. These results are almost similar to that of azo **4c**. The molar ratio and Benesi–Hildebrand methods confirmed the formation of complexes between azo **4c,d** and Fe^{3+} with 1:2 binding stoichiometry. NMR and IR analyses confirmed the coordination between Fe^{3+} and the nitrogen atom of the NH (hydrazone) group and the oxygen atom of the carbonyl (C=O) group. Owing to its good affinity and high sensitivity for Fe^{3+}, azo **4d** showed excellent potential for developing efficient Fe^{3+} chemosensors.

Specification table

Subject area	*Organic Chemistry, Analytical Chemistry and Chemosensors*
Compounds	*(E)-5-(Anthracen-2-yldiazenyl)-2-thioxothiazolidin-4-one and its iron complex*
Data category	*Spectral, synthesized, chemosensing*
Data acquisition format	*^1H NMR, ^{13}C NMR, FT-IR, Elemental analysis, UV-Visible, Fluorometer.*
Data type	*Analyzed*
Procedure	*(E)-5-(Anthracen-2-yldiazenyl)-2-thioxothiazolidin-4-one was synthesized. The interactions of the synthesized compound with Fe^{3+} were investigated using UV/vis, fluorescence, IR and NMR spectrometric analyses.*
Data accessibility	*Data included in the article*

1. Rational

Owing to its impact on several disciplines, developing of efficient sensors for the inspection of metal ions is one of the most popular topics in the chemical researches [1,2]. Recently, there is a strong desire to create amenable methods for

* Corresponding authors.
E-mail addresses: 201450261@uaeu.ac.ae (D. Akram), iaeismail@gelisim.edu.tr (I.A. Elhaty), shaikha.alneyadi@uaeu.ac.ae (S.S. AlNeyadi).

https://doi.org/10.1016/j.cdc.2020.100456
2405-8300/

field testing with emphasis on rapidness, simplicity and low cost [3]. Therefore, sensor developers work aims at achieving aforementioned characteristics. Rhodanine (2-thioxothiazolidine-4-one) and rhodanine azo derivatives play a central role as complexing agents for a large number of transition metal ions and can also be used as analytical reagents [4,5]. Because of these important functions, accurate determination of metal ions in biological systems is essential. Metal complexes are well known for their biological activity [6]. It has been found that the activities of many drugs are increased when they are administered in the form of metal complexes [7,8].

Azo compounds consist of at least one azo chromophore (–N=N–) conjugated with one or more aromatic or heterocyclic system. In industry, these compounds are the most common colorants among the organic dyestuffs [9]. The structural, magnetic, and spectral properties of azo dye complexes have attracted the researchers' interest to design, synthesize, and study the structural characterization of these compounds [10]. As a result, these compounds have been used in many fields such as coloring of several materials, textile fibers dyeing, organic synthesis, and biological/medical studies. In addition, they are used in some advanced applications such as holography, optical storage, nonlinear optics and optical switching [11]. DNA and RNA inhibition, nitrogen fixation, protein synthesis, and carcinogenesis are other applications of azo dyes and their metal complexes as well [11]. Rhodanine based azo compounds have the ability to chelate with several metal ions forming stable six-membered complexes. Iron ions, heavy metal ions, are one of the most important essential trace elements that the human body needs continuously. Fe^{3+} is one of the components of several enzymes and proteins that acts as cofactors for many cellular metabolism reactions [12]. Furthermore, Fe ions are involved in several physiological processes such as transcriptional regulation, oxygen transportation, electron transfer, and oxygen metabolism [13]. In the human body, iron ions are essential for the formation of hemoglobin, and the deficiency of iron can cause anemia [14]. However, high levels of iron may also influence the biological functions because of its ability to catalyze the production of highly reactive oxygen species (ROS) [15]. The production of these species may lead to cancer as well as Alzheimer and Parkinson diseases [16]. Consequently, the U.S. Environmental Protection Agency recommends 5.4 μM as the maximum permitted level of Fe^{3+} in drinking water [15].

Assays for determination of iron levels in the environmental and biomedical analysis remains an active issue. Many methods are used for the detection of Fe^{3+}, such as atomic absorption spectroscopy [17], colorimetric analysis [18], mass spectrometry [19], electrochemical analysis [20], and fluorescence spectroscopic analysis [21]. The design of spectrophotometric sensors for detecting Fe^{3+} has attracted increasing attention owing to their simplicity, high sensitivity, and efficiency. The most effective Fe^{3+} fluorescent probes are limited to organic compounds [21], quantum dots [22,23], and their complexes. We studied in a previous work the synthesis of novel azo rhodanine compounds using a simple and efficient method and studied their application as a potential chemosensor for Fe^{3+} [24]. Herein, we applied the same method to synthesize a new azo rhodanine compound (**4d**). The selectivity of azo (**4d**) for Fe^{3+} cations was studied and compared with compound (**4c**) which showed the best sensitivity and selectivity among our previously synthesized compounds. The structure of this compound was confirmed based on elemental analysis and IR and 1D-NMR spectral data. Furthermore, the interactions of the synthesized compounds with Fe^{3+} were investigated using UV/vis, fluorescence, IR and NMR spectrometric analyses.

2. Procedure

2.1. Chemistry

All of the reagents and chemicals were purchased from Sigma-Aldrich with high purity. The progress of reactions was monitored using Thin Layer Chromatography (TLC). TLC analysis was conducted on silica gel glass plates coated with a fluorescent indicator F_{254} (Fluka) and was visualized under a UV lamp. Column chromatography was conducted using Kieselgel S (silica gel S, 0.063–0.1 mm). Gallenkamp apparatus was used to record the melting points which are uncorrected. Infrared spectra were recorded using the KBr pellet technique on a Thermo Nicolet 470 FT-IR spectrophotometer. ^{1}H-NMR spectra were recorded using DMSO-d_6 as solvents and tetramethylsilane as an internal reference on 400 MHz Varian instruments. Elemental analysis was conducted using a Leco CHN-600 elemental analyzer. UV–vis absorption spectra were obtained using 1.0 cm path length quartz cells on a Cary 50 UV–vis spectrophotometer (Varian, Austria). Fluorescence measurements were conducted using 1.0 cm path length quartz cells on a Cary Eclipse model-3 spectrofluorometer equipped with a high-intensity xenon flash lamp (Varian, Austria).

2.2. Synthesis of rhodanine azo

2.2.1. General procedure

First, 25 mL of aqueous solution of hydrochloric acid (12 M, 32.19 mmol) was added to the appropriate amine compounds **1** (5 mmol). Aqueous solution of sodium nitrite (5.1 mmol in 10 mL of water) was dropped over 10 min into the mixture with stirring in ice bath. Then, a mixture of 2-thioxo-4-thiazolidinone **3** (5 mmol in 25 mL of ethanol) and sodium acetate (5 mmol) was added dropwise to the formed diazonium chloride mixture **2**, over 20 min with cooling at 0-5 °C. The produced slurry mixture was then stirred for 2 h at 5 °C. After that, the mixture was left to stand at room temperature overnight. The dark red precipitate was filtered and washed with water several times. The crude product was recrystallized from hot ethanol to give **4** in a good yield.

2.2.2. (E)-5-(naphthalen-2-yldiazenyl)-2-thioxothiazolidin-4-one (4c)

was synthesized and characterized according to our previous work [24].

2.2.3. (E)-5-(Anthracen-2-yldiazenyl)-2-thioxothiazolidin-4-one (4d)

Dark brown powder; yield 82%; mp 143 °C; R_f 0.50; IR (KBr, cm^{-1}): 3432 (NH), 3049 (C–H aromatic), 2825 (C–H aliphatic), 1716 (C=O), 1629 (C=C), 1473 (N=N), 1200, 1174 (C=S); ^{1}H-NMR [DMSO-d_6, 400 MHz] (δ, ppm): 3.71 (brs, 1H, CH), 7.40–8.85 (m, 9H, aromatic H), 11.25 (brs, 1H, NH, exchanges with D_2O); ^{13}C-NMR [DMSO-d_6, 100 MHz] (δ, ppm): 108.6 (C5-rhodanine), 115.6–145.6 (anthracene carbons), 165.1 (C=O), 204.3 (S=O); Anal. Calcd for $C_{17}H_{11}N_3OS_2$: C, 60.52; H, 3.29; N, 12.45; O, 4.74; S, 19.00; Found: C, 60.92; H, 3.49; N, 12.73; S, 19.05.

2.3. Synthesis of iron (III) metal complex (5c,d)

An ethanolic solution of iron (III) perchlorate was treated with an ethanolic solution of rhodanine dye **4c,d** in a 1:2 molar ratio and refluxed on a water bath for 1 h. The solid complexes were isolated by filtration, washed first with ethanol/acetic acid then ether, and dried in vacuo.

2.3.1. (E)-5-(naphthalen-2-yldiazenyl)-2-thioxothiazolidin-4-one–iron(III) complex (5c)

Dark reddish brown; yield 94%; IR (KBr, cm^{-1}): 3436 (NH), 3050 (C–H aromatic), 2924 (C–H aliphatic), 1624 (C=O), 1529 (C=C), 1432, 1276 (N=N), 1207, 1174 (C=S); ^{1}H-NMR [DMSO-d_6, 400 MHz] (δ, ppm): 7.41-8.00 (m, 7H, aromatic H).

2.3.2. (E)-5-(Anthracen-2-yldiazenyl)-2-thioxothiazolidin-4-one–iron (III) complex (5d)

Dark brown; yield 93%; IR (KBr, cm^{-1}): 3436 (NH), 3050 (C–H aromatic), 2924 (C–H aliphatic), 1624 (C=O), 1529 (C=C), 1432, 1276 (N=N), 1207, 1174 (C=S); ^{1}H-NMR [DMSO-d_6, 400 MHz] (δ, ppm): 7.40–8.85 (m, 9H, aromatic H).

2.4. UV/vis and fluorescence spectral studies

The interaction between azo **4d** and Fe^{3+} was investigated using UV/Vis and fluorescence spectrometry on Cary 50 UV/vis spectrometer and Varian Eclipse spectrofluorometer, respectively. All experiments were performed in DMF. UV/Vis and fluorescence spectra of azo **4d** (3000 µL, 2.50×10^{-5} M) were obtained in the absence and the presence of a four equivalents of iron(III) perchlorate (200 µL, 1.50×10^{-3} M). The solutions were scanned after shaking and incubating for 3 min at room temperature. UV/vis and fluorescence titrations were conducted under the same conditions. Iron(III) perchlorate (1.50×10^{-3} M) was used to titrate azo **4d** (3000 µL, 2.50×10^{-5} M). The solution was mixed well after each addition then incubated for 3 min. The solutions were scanned at room temperature.

2.5. Determination of binding stoichiometry

The binding stoichiometry of azo **4d** with Fe^{3+} was determined using the molar ratio method [25] on a Cary 50 UV/vis spectrophotometer. A solution iron(III) perchlorate (1.50×10^{-3} M) was used to titrate a solution of azo **4d** (2.50×10^{-5} M, 3000 µL) in DMF. The solution was mixed well after each addition then incubated for 3 min, followed by scanning at room temperature. A plot was generated between [Fe^{3+}]/[azo **4d**] and the resulted absorbance at 432 nm.

2.6. Determination of association constant

The association constant, *Ka*, was calculated based on a modified Benesi–Hildebrand equation for 1:2 interactions [26] using UV/vis spectrometry. Iron(III) perchlorate (1.50×10^{-3} M) was used to titrate azo **4d** solution (3000 µL, 2.50×10^{-5} M) in DMF. The solution was mixed well after each addition and was then incubated for 3 min. The solution was scanned at room temperature. *Ka* was calculated following Eq. (1):

$$\frac{1}{A - A_0} = \frac{1}{\left\{K_a (A_{\max} - A_0)[Fe^{3+}]^2\right\}} + \frac{1}{(A_{\max} - A_0)} \quad (1)$$

Here, A_o is azo **4d** (the receptor) absorbance in the absence of Fe^{3+} (the guest), *A* is azo **4d** absorbance in the presence of the added guest (Fe^{3+}), A_{max} is azo **4d** absorbance in the presence of [Fe^{3+}]max, and *Ka* is the association constant (M^{-1}). A plot was generated between $1/[Fe^{3+}]^2$ and $1/(A - A_o)$. *Ka* is calculated by intercept/slope.

2.7. Determination of limit of detection (LOD)

Limit of detection (LOD) was calculated using IUPAC 3σ criteria on UV/vis spectrophotometer. The standard deviation of the blank was determined by scanning the blank solution of azo **4d** (3000 µL, 2.50×10^{-5} M) in DMF five times. Then, such solution was titrated with a solution of iron(III) perchlorate (1.50×10^{-3} M). The solution was mixed well after each addition and was then incubated for 3 min. The solution is scanned at room temperature.

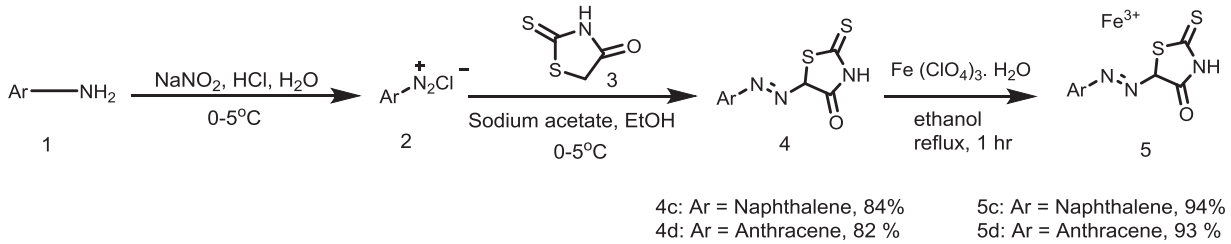

Scheme 1. Synthesis of rhodanine-based azo dye **4c,d** and their iron (III) complexes **5c,d**.

A linear calibration curve was plotted between the absorbance and the concentration of Fe^{3+} ions. LOD was calculated as follows:

$$LOD = 3\sigma \quad (2)$$

$$\sigma = SD/s \quad (3)$$

Here, s is the slope of the obtained calibration curve and SD is the standard deviation of azo **4d** blank solution.

3. Results and discussion

3.1. Synthesis

The structure of compound **4d** was identified using FT-IR, ^{1}H-NMR, and ^{13}C-NMR spectroscopy, and elemental analysis. In the IR spectra of compound **4d**, peaks were observed near 1704 and 1716 cm^{-1}, which are attributable C=O bonds, and at 1253 and 1200 cm^{-1}, which are attributable to C=S bond stretching. Additionally, the appearance of new bands in the region of 1487 and 1473 cm^{-1}, which are attributable to azo N=N bond stretching, confirmed the successful formation of compound 4**d**. The ^{1}H-NMR spectrum of compound **4d** showed a signal at δ = 11.25 ppm, corresponding to the exchange between D_2O and the amino group. The broad singlet at δ = 3.71 ppm, integrated as one proton, corresponded to H5-rhodanine. In the ^{13}C-NMR spectrum, rhodanine C5 resonated at δ = 108.6 ppm, the carbonyl group appeared at δ = 165.1 ppm, and the C=S group resonated at δ = 204.3 ppm Scheme 1.

3.2. Spectroscopic analysis

3.2.1. Response time of azo 4d

The response time of azo **4d** towards Fe^{3+} metal ion in solution was determined in order to evaluate its sensitivity towards Fe^{3+}. A mixture of azo **4d** (2.5×10^{-5} M) and four equivalents of Fe^{3+} in DMF was prepared. The absorbance and fluorescence intensity change of azo **4d** was recorded over time. The absorbance and fluorescence intensities of azo **4d** reached maximum values and stabilized after 3 min. Therefore, the incubation time was fixed by 3 min in all experiments to ensure sufficient time for chelation of Fe^{3+} with azo **4d**. The obtained response time of azo **4d** was exactly similar to that of azo **4c** towards Fe^{3+}.

3.2.2. UV/vis and fluorescence studies

The interactions between azo **4c,d** and Fe^{3+} in DMF were studied using UV/vis and fluorescence spectrometric techniques. As mentioned in our previous work, azo **4c** showed an absorbance band at 403 nm (ε = 9360 M^{-1} cm^{-1}), which is attributed to the π–π^* transition. Similarly, azo **4d** showed an absorbance band at 432 nm (13440 M^{-1} cm^{-1}) attributed to π–π^* transition while n–π^* transitions in both compounds were not easy to identify. However, azobenzene compounds shows a band with high intensity at ca 350 nm and a low intense band at ca 440 nm (is not easy to identify) attributed to π–π^* and n–π^* transitions respectively [27]. The bathochromic shift observed for azo **4d** is attributed to extended conjugation resulting from the additional benzene ring in anthracene. Upon the addition of four equivalents of Fe^{3+}, the absorbances of these bands for both compounds increased without any shift in the peak position and without an obvious change of the peak shape, as shown in Fig. 1, indicating that Fe^{3+} interacts with azos **4c** and **4d**. These changes of absorption spectra indicated the direct binding of Fe^{3+} to azos **4c** and **4d** without affecting their structure. Furthermore, the interactions between azo **4c,d** and Fe^{3+} were studied using fluorescence spectrometry. Upon excitation of azo **4c** at 395 nm, two significant bands were observed in the emission spectrum at 374 and 423 nm. In contrast, upon excitation of azo **4d** at 350 nm, a single emission band was observed at 369 nm (Fig. 2). Upon addition of Fe^{3+}, the fluorescence intensities of azos **4c** and **4d** were quenched without a shift in the peak position. In general, paramagnetic ions such as Cu^{2+}, Co^{2+}, Ni^{2+}, and Fe^{3+} may induce the quenching of the fluorescence intensity of a fluorophore attached to them through two different mechanisms, photoinduced metal-to-fluorophore electron transfer or electronic energy transfer [28,29]. The fluorescence intensity of azos **4c** and **4d** was quenched with addition of Fe^{3+} indicated that the added Fe^{3+} interacted with the azos **4c** and **4d**

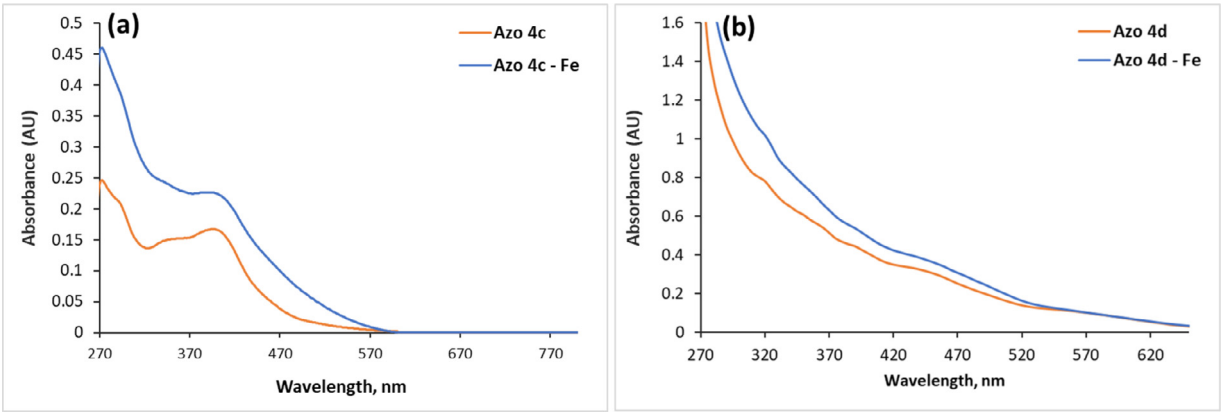

Fig. 1. UV/vis absorption spectra of (a) azo **4c** (2.5×10^{-5} M) and (b) azo **4d** (2.5×10^{-5} M) before and after addition of 4 equiv. of Fe^{3+} in DMF.

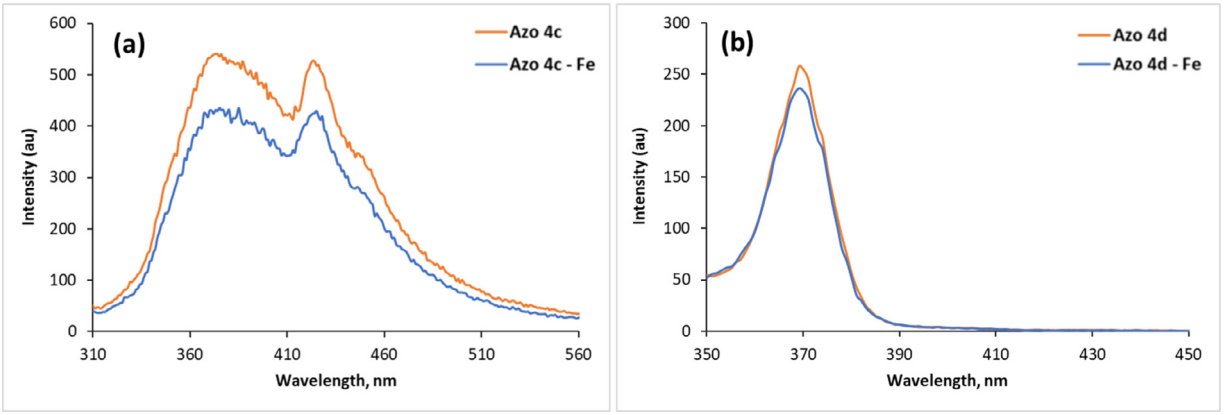

Fig. 2. Fluorescence spectra of (a) azo **4c** (2.5×10^{-5} M) and (b) azo **4d** (2.5×10^{-5} M) before and after addition of 4 equiv. of Fe^{3+} in DMF.

which confirmed the results obtained from UV-vis spectroscopy. It has been reported that the fluorescence quenching mechanism of Fe^{3+} occurs via electron or energy transfer [30]. Azos **4c** and **4d** possess amino and carboxyl function groups and Fe^{3+} have shown preferentially binding with nitrogen and oxygen atoms of imino and carbonyl groups respectively [21,31]. Therefore, we speculated that nitrogen atom of imino group and oxygen atom of carbonyl group in the azos **4c** and **4d** molecules might donate electrons to Fe^{3+} ions. Other azos **4c** and **4d** molecules may occupy the other interaction sites of the six-coordinated Fe^{3+} ion. Consequently, the produced coordination interactions induced intra-particles cross links which resulted in the fluorescence quenching [32] as shown in Fig. 8.

3.2.3. Binding stoichiometry

The binding stoichiometry between azo **4d** and Fe^{3+} was estimated using the molar ratio method. Azo **4d** in DMF was titrated with Fe^{3+} and plots of [Fe^{3+}]/[azo **4d**] versus absorbance were generated using its absorbance at 432 nm. As shown in Fig. 3, the stoichiometry between azo **4d** and Fe^{3+} was 1:2, indicating that both azo **4d** formed a (M_2L) complex structure. Azos **4c** and **4d** have the same stoichiometry with Fe^{3+} because they have the same number of binding sites as shown in Fig. 8.

3.2.4. Association constant

To elucidate the binding strength between azo **4d** and Fe^{3+}, the binding affinity of Fe^{3+} towards azo **4d** was determined using the Benesi–Hildebrand plot (Eq. (1)) based on a 1:2 molar ratio. As shown in Fig. 4, good linearity was obtained with $R^2 = 0.9868$ and linear regression equations of $y = 3 \times 10^{-8}x + 14.412$ for azo **4d**. The linearity of these plots confirmed a 1:2 stoichiometry for azo **4d** with Fe^{3+}, as observed using the molar ratio method [33]. The association constant was calculated to be 5.35×10^8 M^{-1} for azo **4d**. This value is slightly higher than that of azo **4c** (4.63×10^8 M^{-1}). Thus, Fe^{3+} showed a high binding affinity towards both compounds, compared with the binding affinities of some reported receptors which showed significant selectivity towards Fe^{3+} [34,35]. For instance, the obtained association constant for rhodamine B and thiocarbonyl moieties was 2.75×10^4 M^{-1} [36], while it was 1.52×10^4 M^{-1} for another rhodamine B derivative [37]. In addition, it ranged between 7.72×10^4 and 1.21×10^5 M^{-1} for azo-Schiff base receptors holding azo and azomethine groups [37].

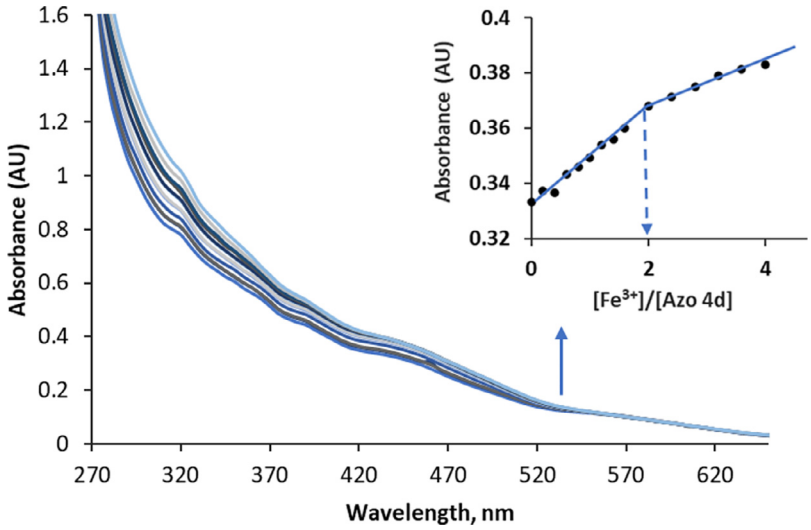

Fig. 3. UV/vis titration of azo **4d** (2.5×10^{-5} M) before and after addition of Fe^{3+} (4 equiv) in DMF. Inset: Molar ratio method for determination of the binding stoichiometry of azo **4d** with Fe^{3+} (4 equiv).

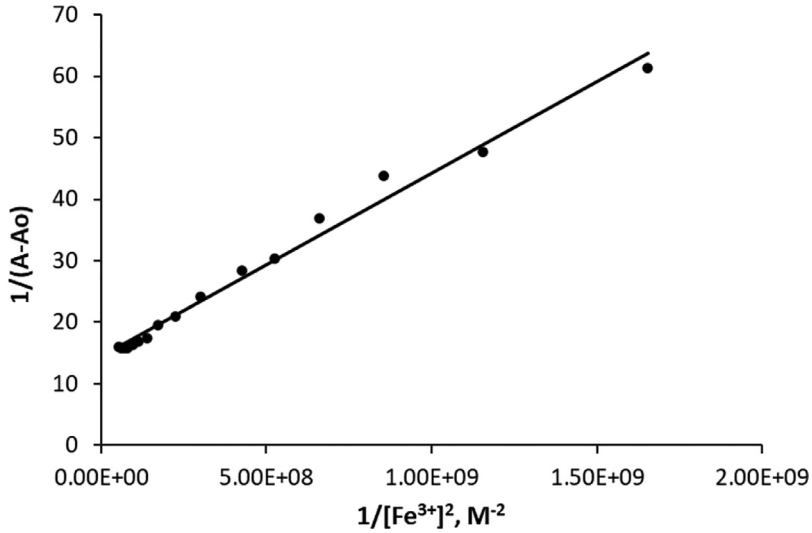

Fig. 4. Benesi–Hildebrand plot of azo **4d** with Fe^{3+} (based on 1:2 binding stoichiometry).

3.2.5. Limit of detection (LOD)

LOD of azo **4d** towards Fe^{3+} was calculated based on UV/vis calibration curve using Eqs. (2) and (3). The LOD of azo **4d** towards Fe^{3+} was 7.05 µM, as shown in Fig. 5. The LOD of azo **4d** is slightly higher than that of azo **4c** (5.14 µM), indicating that azo **4c** is slightly more sensitive to Fe^{3+} than azo **4d**. As azos **4c** and **4d** have the same binding mode, this small difference may be attributed to the small differences in the chemical structures of these compounds. A comparison of our azos probes with some of the previously reported on Fe^{3+} chemosensors in terms of their LOD values can be said that these values were acceptable values as much as the values reported in the literature. For instance, 1,10-phenanthroline complexes showed LOD of 1.61×10^{-5} M [38], while azo-Schiff base complexes including azo and azomethine groups showed 6.44×10^{-6} M [35].

3.2.6. ^{1}H NMR analysis

^{1}H NMR spectral studies were conducted to verify the formation of the complexes between rhodanine dyes (**4c,d**) and Fe^{3+}. The ^{1}H NMR spectrum of free azo **4c** (Fig. 6B) shows peaks corresponding to the naphthalene protons at δ = 7.94-8.89 ppm integrated as seven protons. The broad NH singlet is located downfield at 11.38 ppm. In contrast, the spectrum for free azo **4d** (Fig. 7B) shows peaks corresponding to the anthracene protons at δ = 7.49-8.83 ppm integrated as nine protons. The broad NH singlet is located downfield at 11.34 ppm. For the paramagnetic iron(III) complexes of the azo dyes (**5c,d**), the signals for the aromatic protons of the naphthalene and anthracene rings are broader and shifted upfield (δ = 7.41-8.00 ppm

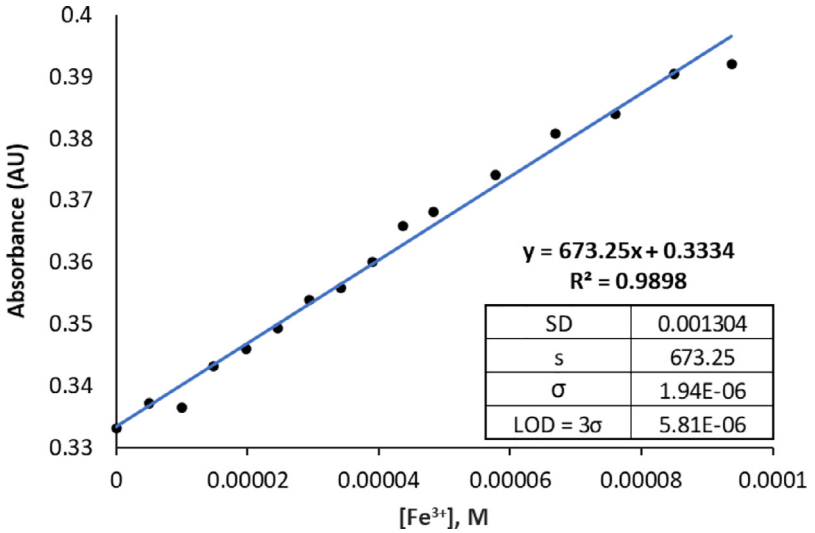

Fig. 5. Calibration curve for the absorbance of azo **4d** as a function of [Fe^{3+}].

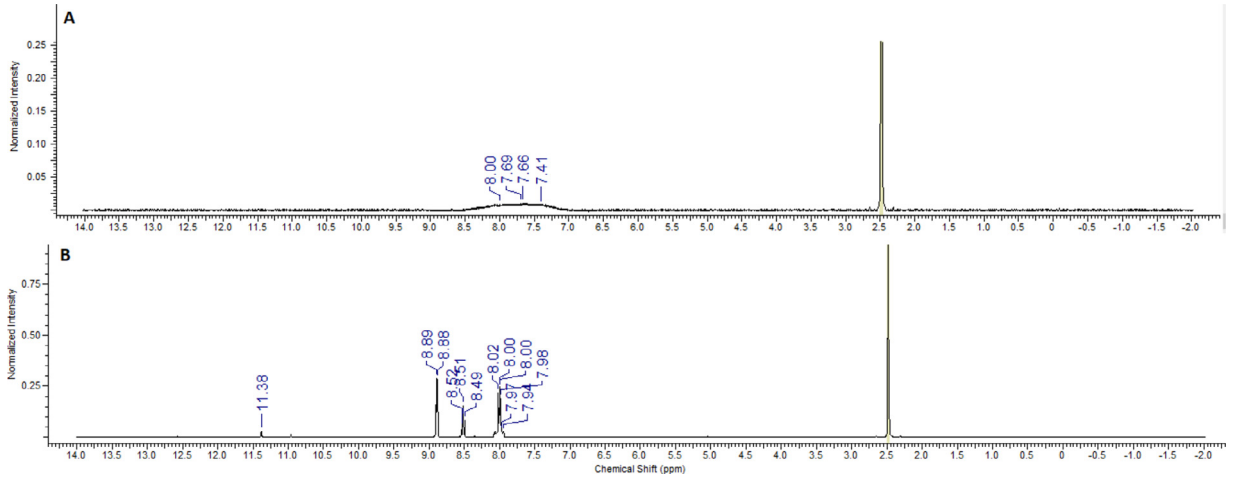

Fig. 6. ^{1}H-NMR spectra of (A) Fe^{3+}–azo complex **5c** and (B) free azo **4c** in DMSO-d_6 at 298 K.

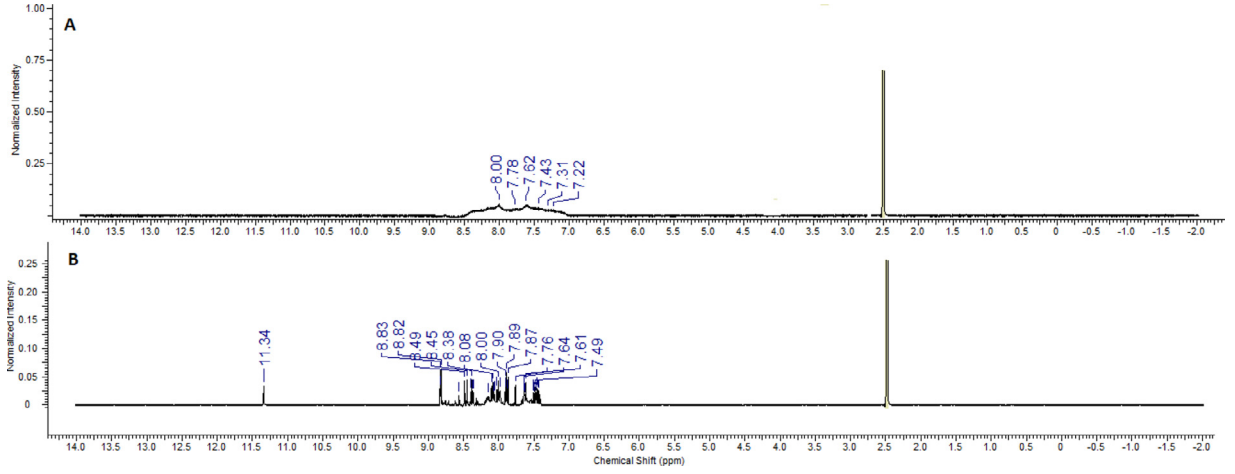

Fig. 7. ^{1}H-NMR spectra of (A) Fe^{3+}–azo complex **5d** and (B) free azo **4d** in DMSO-d_6 at 298 K.

Table 1
Characteristic IR bands of azo dyes **4c** and **4d** and their iron(III) complexes **5c** and **5d**

Functional Group	Wavenumber (cm^{-1}) 4c	5c	4d	5d
υ(C=O)	1704	1624	1716	1627
υ(C=S)	1210, 1171	1207, 1174	1200, 1174	1203, 1173
υ(N=N)	1487		1431	
υ(HC=N)	-	1431	-	1431
υ(=N–NH)	-	1276	-	1276

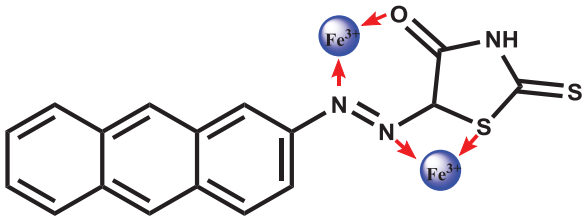

Fig. 8. Chemical structure of the rhodanine azo–iron complex.

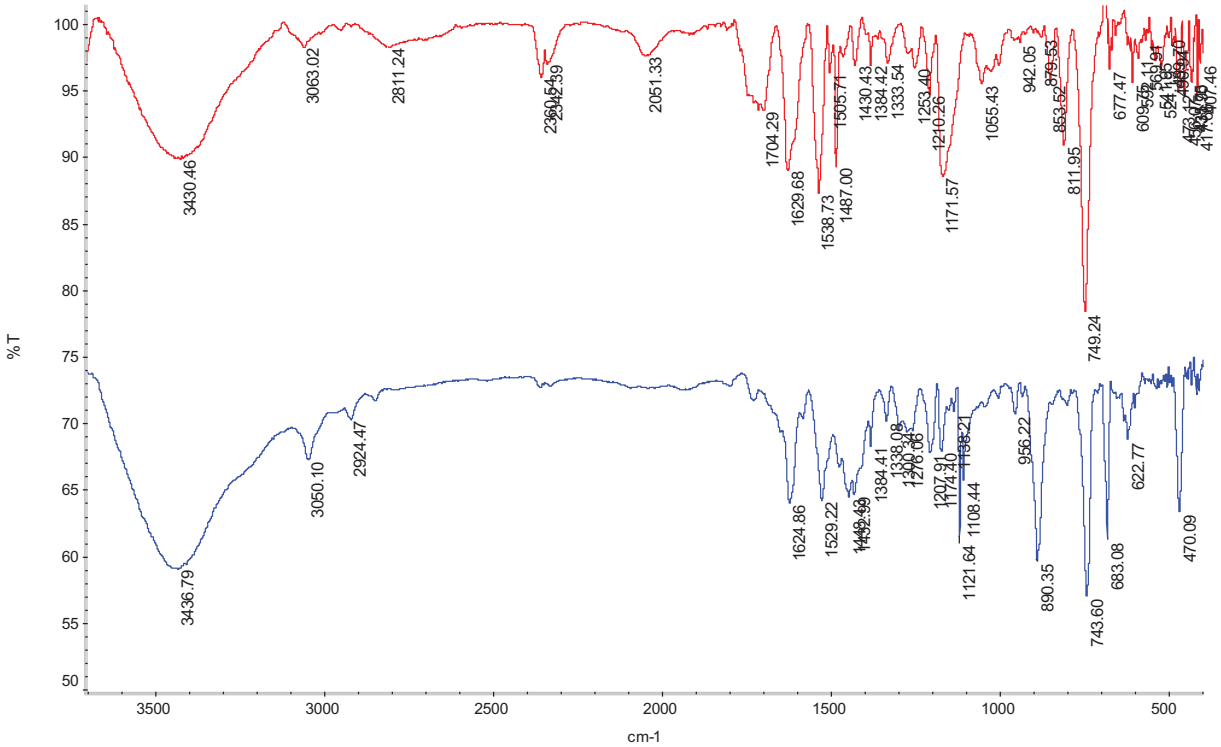

Fig. 9. IR spectra of azo dye **4c** (top) and Fe^{3+}–azo complex **5c** (bottom).

in **5c** and δ = 7.22-8.00 ppm in **5d** owing to disruption of the ring current by interactions between the aromatic groups and Fe^{3+}. Furthermore, complexation results in the disappearance of the NH signal.

3.2.7. IR analysis

IR spectroscopy is a useful tool in investigating and identifying functional groups in organic compounds. The characteristic IR absorption bands in the spectral range between 4000 and 400 cm^{-1} were determined for the free azo dyes and the complexes (Table 1). The coordination modes between the azo dyes and Fe^{3+} (Fig. 8) were assigned by comparison of the IR spectra of the iron(III) complexes with those of the free azo dyes (Figs. 9 and 10). The following features should be noted: the band near 1684 cm^{-1} assigned to υ(C=O) in the IR spectrum of azo **4d** shifted considerably towards lower energies in the IR spectrum of complex **5d** (1627 cm^{-1}). This shift indicates that the coordination of the azo dye to the Fe^{3+}metal

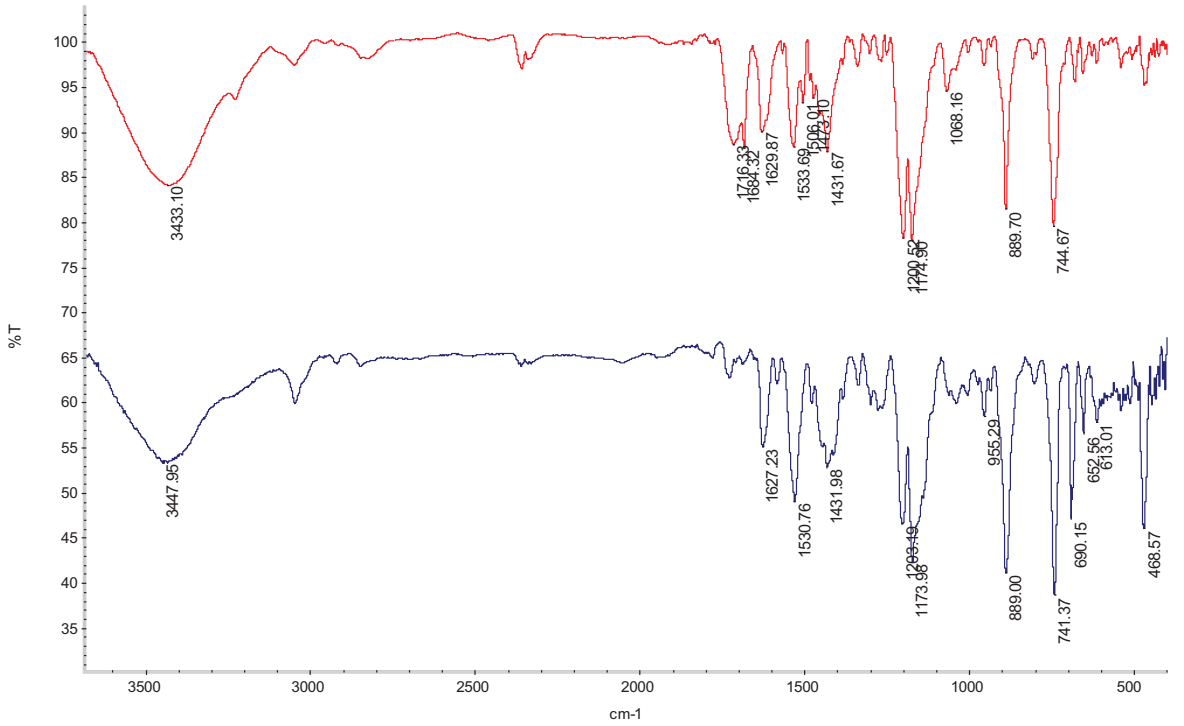

Fig. 10. IR spectra of (a) azo dye **4d** (top) and Fe3+–azo complex **5d** (bottom).

center occurs through oxygen and that the carbonyl oxygen group participates in chelation [22]. The splitting of the υ(N=N) band in azo **4d** into two bands near 1431 and ~1276 cm^{-1} in complex **5d** is due to υ(HC=N) and υ(=N–NH) of hydrazone, respectively, which provides evidence for the participation of the hydrazone N in chelation after deprotonation, leading to the formation of a covalent linkage. Furthermore, complex **5d** exhibits new bands near 690 and 468 cm^{-1}, which were assigned to the formation of Fe–O and Fe–N bonds, respectively. This finding further indicates that the coordination involves the nitrogen atom of the NH (hydrazone) group and the oxygen atom of the carbonyl (C=O) group. The ν(C=S) stretching band of the azo dye at 1200 and 1174 cm^{-1} remains practically unchanged in the complex, confirming that Fe^{3+} is not coordinated to the sulfur atom in C=S. The $\nu(C_5\text{-}S_4)$ frequency decrease from 744 cm^{-1} to 741 cm^{-1} in **5d** and from 749 cm^{-1} to 743 cm^{-1} in **5c** the suggest the coordination of the ligands through the ring sulphur atom (C_5-S_4). Similar results were obtained for complex **5c**.

4. Conclusions

In conclusion, synthesis of rhodanine-based azo dye (**4d**) was confirmed using IR, ^{1}H-NMR, ^{13}C-NMR and CHN-elemental analysis techniques. UV/vis, fluorescence, IR, and NMR analyses confirmed the interaction between azo **4c,d** and Fe^{3+} with 1:2 stoichiometry. The new synthesized azo **4d** compound showed high selectivity (binding constant of 5.35×10^{8} M^{-1}) and sensitivity (LOD of 7.05 μM) towards Fe^{3+} ions almost similar to that of azo **4c**. NMR and IR analysis confirmed the coordination between Fe^{3+} and the nitrogen atom of the NH (hydrazone) group and the oxygen atom of the carbonyl (C=O) group.

Authors' contribution

Conceptualization, S.S.A. and I.A.E.; Methodology, D.A.; Original Draft Preparation, Writing—Review & Editing, S.S.A. and I.A.E.

Funding

This research did not receive any specific grant from funding agencies in the public, commercial, or not-for-profit sectors.

Declaration of Competing Interest

The authors declare no competing interests.

Acknowledgments

The authors are grateful to the Merck Company for the providing with chemicals assistance.

Supplementary materials

Supplementary material associated with this article can be found, in the online version, at doi:10.1016/j.cdc.2020.100456.

References

[1] A.A. El-Kady, M. Abdel-Wahhab, Occurrence of trace metals in foodstuffs and their health impact, Trends Food Sci. Technol. 75 (2018) 36–45, doi:10.1016/j.tifs.2018.03.001.
[2] S. Khalid, M. Shahid, B.I. Natasha, T. Sarwar, A.H. Shah, N.K. Niazi, A review of environmental contamination and health risk assessment of wastewater use for crop irrigation with a focus on low and high-income countries, Int. J. Environ. Res. Public Health 15 (2018) 895–931, doi:10.3390/ijerph15050895.
[3] J. Rull-Barrull, M. d'Halluin, E. Le Grognec, F.X. Felpin, Chemically-modified cellulose paper as smart sensor device for colorimetric and optical detection of hydrogen sulfate in water, Chem. Commun. 52 (2016) 2525–2528, doi:10.1039/C5CC09889K.
[4] S.B. Savvin, R.F. Gur'eva, 5-Axo derivatives of rhodanine and its analogues in the analytical chemistry of the noble metals, Talanta 34 (1987) 87, doi:10.1016/0039-9140(87)80012-7.
[5] V. Anger, S. Ofri, Glutaconaldehyd als Tüpfelreagens. III, Microchim. Acta 52 (1964) 987–989, doi:10.1007/BF01224562.
[6] M. Sathya, Ind. J. Exp. Bio. (1994) 279 Retrieved from http://nopr.niscair.res.in/handle/123456789/39 .
[7] P.N. Gupata, A. Raina, V.K. Bhat, Polarographic reduction of aromatic azo compounds, Asian J. Chem. 2 (1990) 73 Retrieved from http://www.asianjournalofchemistry.co.in/user/journal/viewarticle.aspx?ArticleID=2_1_11 .
[8] M. Kodama, Thermodynamic study of formation reactions of mercury(II) complexes with polyamino polycarboxylic macrocycles, Bull. Chem. Soc. 67 (1994) 2990, doi:10.1246/bcsj.67.2990.
[9] K. Hunger, Industrial Dyes: Chemistry, Properties, Applications, Wiley-VCH, Weinheim, 2003, doi:10.1002/3527602011.
[10] E.A. Geary, L.Y. Yellowlees, L.A. Jack, I.H. Oswald, S. Parsons, N. Hirata, J.R. Durrant, N. Robertson, Synthesis, structure, and properties of [Pt(II)(diimine)(dithiolate)] dyes with 3,3′-, 4,4′, and 5,5′-disubstituted bipyridyl: applications in dye-sensitized solar cells, Inorg. Chem. 44 (2005) 242, doi:10.1021/ic048799t.
[11] A. Abdelaziz, H.A Elbadawy, Spectral, electrochemical, thermal, DNA binding ability, antioxidant and antibacterial studies of novel Ru(III) Schiff base complexes, Spectrochim. Acta A 124 (2014) 404, doi:10.1016/j.saa.2014.01.050.
[12] J. Wang, K. Pantopoulos, Regulation of cellular iron metabolism, Biochem. J. 434 (2011) 365, doi:10.1042/bj20101825.
[13] C.R. Lohani, K.H. Lee, The effect of absorbance of Fe^{3+} on the detection of Fe^{3+} by fluorescent chemical sensors, Sens. Actuators B Chem. 143 (2010) 649–654, doi:10.1016/j.snb.2009.10.004.
[14] L.H. Allen, Iron supplements: scientific issues concerning efficacy and implications for research and programs, J. Nutr. 132 (2002) 813S, doi:10.1093/jn/132.4.813S.
[15] J.A. Ho, H.C. Chang, W.T. Su, DOPA-mediated reduction allows the facile synthesis of fluorescent gold nanoclusters for use as sensing probes for ferric ions, Anal. Chem. 84 (2012) 3246, doi:10.1021/ac203362g.
[16] L. Zecca, M.H. Youdim, P.C. Riederer Jr., R.R. Crichton, Iron, brain ageing and neurodegenerative disorders, Nat. Rev. Neurosci. 5 (2004) 863, doi:10.1038/nrn1537.
[17] M. Ghaedi, K. Mortazavi, M. Montazerozohori, A. Shokrollahi, M Soylak, Flame atomic absorption spectrometric (FAAS) determination of copper, iron and zinc in food samples after solid-phase extraction on Schiff base-modified duolite XAD 761, Mater. Sci. Eng. C. Mater. Biol. Appl. 33 (2013) 2338–2344, doi:10.1016/j.msec.2013.01.062.
[18] Y. Ma, J. Thiele, L. Abdelmohsen, J. Xu, W.T. Huck, Biocompatible macro-initiators controlling radical retention in microfluidic on-chip photopolymerization of water-in-oil emulsions, Chem. Commun. 50 (2014) 112, doi:10.1039/c3cc46733c.
[19] A. Bobrowski, K. Nowak, J. Zarebski, Application of a bismuth film electrode to the voltammetric determination of trace iron using a Fe(III)-TEA-BrO_3-catalytic system, Anal. Bioanal. Chem. 382 (2005) 1691–1697, doi:10.1007/s00216-005-3313-2.
[20] A. Sil, V.S. Ijeri, A.K. Srivastava, Coated-wire iron(III) ion-selective electrode based on iron complex of 1,4,8,11-tetraazacyclotetradecane, Sens. Actuators B Chem. 106 (2005) 648–653, doi:10.1016/j.snb.2004.09.013.
[21] M.H. Lee, T.V. Giap, S.H. Kim, Y.H. Lee, C. Kang, J.S. Kim, A novel strategy to selectively detect Fe(III) in aqueous media driven by hydrolysis of a rhodamine 6G Schiff base, Chem. Commun. 46 (2010) 1407–1409, doi:10.1039/B921526C.
[22] T. Noipa, K. Ngamdee, T. Tuntulani, W. Ngeontae, Cysteamine CdS quantum dots decorated with Fe^{3+} as a fluorescence sensor for the detection of PPi, Spectrochim. Acta A Mol. Biomol. Spectrosc. 118 (2014) 17, doi:10.1016/j.saa.2013.08.067.
[23] T. Jamieson, R. Bakhshi, D. Petrova, R. Pocock, M. Imani, A.M. Seifalian, Biological applications of quantum dots, Biomaterials 28 (2007) 4717, doi:10.1016/j.biomaterials.2007.07.014.
[24] D. Akram, I.A. Elhaty, S.S. AlNeyadi, Synthesis and antibacterial activity of rhodanine-based azo dyes and their use as spectrophotometric chemosensor for Fe^{3+} ions, Chemosensors 8 (2020) 16, doi:10.3390/chemosensors8010016.
[25] Y. Marcus, On the use of the molar ratio method for determining association stoichiometry, Isr. J. Chem. 5 (1967) 143–149, doi:10.1002/ijch.196700028.
[26] R. Ghanem, F. Yousef, O. Abu Awwad, Effect of pH and β -cyclodextrin on the photophysical properties of lamotrigine, Turk. J. Chem. 42 (2018) 247–256, doi:10.3906/kim-1706-12.
[27] A. Natansohn, P. Rochon, Photoinduced motions in azo-containing polymers, Chem. Rev. 102 (41) (2002) 39–76, doi:10.1021/cr970155y.
[28] S. Pal, N. Chatterjee, P.K. Bharadwaj, Selectively sensing first-row transition metal ions through fluorescence enhancement, RSC Adv. 4 (2014) 26585–26620, doi:10.1039/C4RA02054E.
[29] A.W. Varnes, R.B. Dodson, E. Wehry, Interactions of transition-metal ions with photoexcited states of flavines. Fluorescence quenching studies, J. Am. Chem. Soc. 94 (1972) 946–950, doi:10.1021/ja00758a037.
[30] J. Li, Q. Wang, Z. Guo, H. Ma, Y. Zhang, B. Wang, D. Bin, Q. Wei, Highly selective fluorescent chemosensor for detection of Fe^{3+} based on Fe_3O_4@ZnO, Sci. Rep. 6 (2016) 23558–23566, doi:10.1038/srep23558.
[31] A.J. Weerasinghe, F.A. Abebe, E. Sinn, Rhodamine based turn-ON dual sensor for Fe^{3+} and Cu^{2+}, Tetrahedron Lett. 52 (2011) 5648–5651, doi:10.1016/j.tetlet.2011.08.092.
[32] X. Yuan, Z. Luo, Y. Yu, Q. Yao, J. Xie, Luminescent noble metal nanoclusters as an emerging optical probe for sensor development, Chem. Asian J. 8 (2013) 858–871, doi:10.1002/asia.201201236.
[33] Y. Shiraishi, S. Sumiya, Y. Kohno, T. Hirai, A rhodamine–cyclen conjugate as a highly sensitive and selective fluorescent chemosensor for Hg(II), J. Org. Chem. 73 (2008) 8571–8574, doi:10.1021/jo8012447.
[34] K. Kaur, S. Chaudhary, S. Singh, S.K. Mehta, Highly selective probe based on imine linkage for Zn^{2+} and HSO_3^- in mixed aqueous media, J. Lumin. 160 (2015) 282–288, doi:10.1016/j.jlumin.2014.12.035.
[35] Ö. Özdemir, Synthesis of novel azo linkage-based Schiff bases including anthranilic acid and hexanoic acid moieties: investigation of azo-hydrazone and phenol-keto tautomerism, solvatochromism, and ionochromism, Turk. J. Chem. 43 (2019) 266–285, doi:10.3906/kim-1807-24.

[36] Y. Fu, X.X. Pang, Z.Q. Wang, Q. Chai, F. Ye, A highly sensitive and selective fluorescent probe for determination of Cu (II) and application in live cell imaging, Spectrochim. Acta A Mol. Biomol. Spectrosc. 208 (2019) 198–205, doi:10.1016/j.saa.2018.10.005.
[37] H. Chen, X. Bao, H. Shu, B. Zhou, R. Ye, J. Zhu, Synthesis and evaluation of a novel rhodamine B-based 'off-on' fluorescent chemosensor for the selective determination of Fe^{3+} ions, Sen. Actuators B Chem. 242 (2017) 921–931, doi:10.1016/j.snb.2016.09.163.
[38] L. Kozak, P. Niedzielski, W. Wachowiak, The tandem analytical method of flow injection diode array spectrophotometry and flame atomic absorption spectrometry (FI-DAD(vis)-FAAS) in iron speciation studies using 1,10-phenanthroline complexes, Microchem. J. 110 (2013) 54–60, doi:10.1016/j.microc.2013.02.004.